

–Supporting Information for the manuscript entitled–

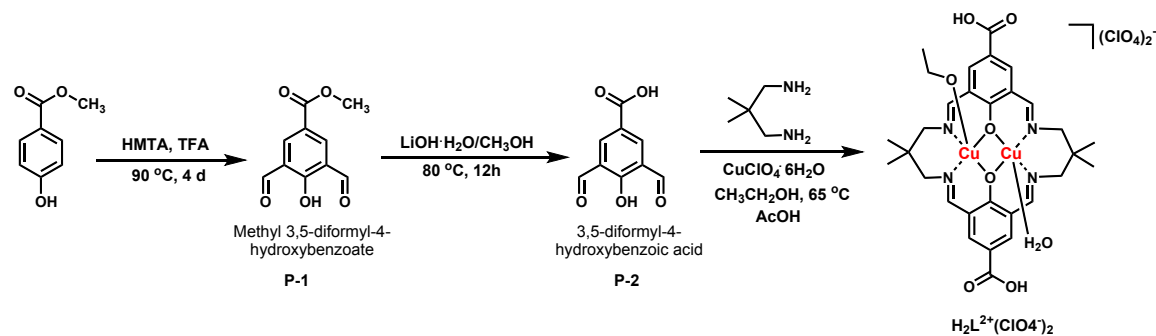
**“A rare 4-fold interpenetrated metal-organic framework constructed from an anionic indium-based node and a cationic dicopper linker”**

Sreenath Pappuru,<sup>a</sup> Karam B. Idrees,<sup>b</sup> Zhijie Chen,<sup>b</sup> Dina Shpasser<sup>a</sup> and Oz M. Gazit<sup>\*a</sup>

*ozg@technion.ac.il*

Wolfson Department of Chemical Engineering  
Technion-Israel Institute of Technology,  
*Haifa-3200003, Israel*

### Synthesis of $H_2L^{2+}(ClO_4^-)_2$ :



**Scheme S1** Synthetic route for  $H_2L^{2+}(ClO_4^-)_2$

Compounds P-1 and P-2 were synthesized with slight modification to a previously reported procedure.<sup>1,2</sup>

#### Methyl 3,5-diformyl-4-hydroxybenzoate

A mixture of methyl 4-hydroxybenzoate (12 g, 79 mmol) and hexamethylenetetramine (45.6 g, 325 mmol) was dissolved in anhydrous TFA (90 ml). The obtained yellow solution was heated under reflux for 4 d, to obtain a viscous dark-orange solution. 530 ml  $H_2O$  were added and the mixture was heated up to give a homogeneous solution. Upon cooling, the product precipitated slowly from the solution (yield: 12.15g, 74 %).  $^1H$  NMR (400 MHz,  $CDCl_3$ )  $\delta$  12.05 (s, 1H), 10.27 (s, 2H), 8.65 (s, 2H), 3.96 (s, 3H).

#### 3,5-diformyl-4-hydroxybenzoic acid:

A mixture of methyl 3,5-diformyl-4-hydroxybenzoate (5 g, 24 mmol) and  $LiOH \cdot H_2O$  (8.43 g, 201 mmol) was added to a flask containing 500 mL  $H_2O$  and 125 ml methanol. The solution was refluxed at 80 °C overnight to yield a yellow solution. Subsequently, the methanol was evaporated by rotary evaporation and a 6N HCl solution was added until the pH=2. The obtained light-yellow precipitate, was filtered out and dried under vacuum (yield: 4.42 g, 95 %).  $^1H$  NMR (400 MHz,  $DMSO-d_6$ )  $\delta$  13.31 (bs, 1H), 12.12 (bs, 1H), 10.28 (s, 2H), 8.54 (s, 2H).

### Synthesis of $H_2L^{2+}(ClO_4^-)_2$ :

The dicopper Robson-type ligand  $H_2L^{2+}(ClO_4^-)_2$  was synthesized with slight modification to a previously reported procedure.<sup>2</sup> In a 20 ml vial, 3,5-diformyl-4-hydroxybenzoic acid (40 mg, 0.2 mmol) was dissolved in 6 ml hot ethanol. 100 mg  $Cu(ClO_4^-)_2 \cdot 6H_2O$  (0.27 mmol), 23  $\mu$ L  $CH_3COOH$  (0.4 mmol) and 21 mg 2,2-dimethyl-1,3-propanediamine (0.2 mmol) in 4 ml ethanol were added to the aldehyde solution. After addition, the vial was sealed and heated to 65 °C for 3 days. Prism like dark green crystals were collected and dried. (Yield: 0.147 g, 81 %). ATR IR ( $cm^{-1}$ ):  $\nu$ (amine C–H), 2967-2865;  $\nu$ (COOH), 1679;  $\nu$ (C=N), 1638;  $\nu$ ( $ClO_4^-$ ), 1072 and 621. MS (ESI): m/z 745 [ $H_2L^{2+}ClO_4^-$ ].

### Synthesis of TIF-1:

27 mg ligand, 2 mg  $In(NO_3)_3 \cdot xH_2O$ , DMF(3 ml),  $CH_3CN$ (2 ml) and  $HNO_3$  (0.2 ml, 2.7M in DMF) were added to a 20 ml vial and the vial was sealed and placed in an 80 °C oven for 5 d, green prism like crystals of TIF-1 were collected and air dried, 72 % Yield. ATR IR ( $cm^{-1}$ ):  $\nu$  ( $H_2O$ ),

3385;  $\nu$  (amine C–H), 2961-2871;  $\nu$  (C=N), 1642;  $\nu$  (COO), 1578, 1316;  $\nu$  ( $\text{NO}_3^-$ ), 1402. In addition, we note that during MOF synthesis optimization, we have also tried different temperatures (80, 90, 100 and 110 °C), several metal ions (ligand:  $\text{In}(\text{NO}_3)_3 = 1:1, 1:2, 1:2.5, 1:3, 1:4, 1.5:1, 2:1, 3:1, 4:1$  and  $5:1$ ) and modulator concentrations (0.5M, 1M, 1.5M, 2M and 2.7M  $\text{HNO}_3$ , Acetic acid in DMF) to synthesize heterometallic MOF's. Only the above mentioned optimal temperature (80 °C) and ideal ratio of starting materials (ligand:  $\text{In}(\text{NO}_3)_3 = 5.6:1$ ) yielded **TIF-1** product. The other ratio of starting materials and temperature yielded amorphous products, which was confirmed from PXRD analysis.

#### **X-ray crystallographic measurements:**

The single-crystal material was immersed in Paratone–N oil and mounted on a APEX II Bruker diffractometer at 200K. Data collection was performed using monochromated Mo  $K\alpha$  radiation,  $\lambda = 0.71073 \text{ \AA}$ , using  $\phi$  and  $\omega$  scans to cover the Ewald sphere. Accurate cell parameters were obtained with the amount of indicated reflections. The structure was solved with the Olex2<sup>3</sup> software using the olex2.solve<sup>4</sup> structure solution program, applying charge flipping, and refined with the ShelXL<sup>5</sup> refinement package using Least Squares minimization. All non-hydrogen atoms were refined with anisotropic displacement parameters. The hydrogen atoms were refined isotropically on calculated positions using a riding model with their  $U_{\text{iso}}$  values constrained to 1.5 times the  $U_{\text{eq}}$  of their pivot atoms for terminal  $\text{sp}^3$  carbon atoms and 1.2 times for all other carbon atoms. Mercury 3.10.1 software was used for molecular graphics.<sup>6</sup>

The X-ray crystallographic coordinates for structures  $\text{H}_2\text{L}^{2+}(\text{ClO}_4^-)_2$  and **TIF-1** reported in this article have been deposited at the Cambridge Crystallographic Data Centre (CCDC), under deposition number CCDC 2039820-2039821.

#### **Supercritical drying procedure<sup>7</sup>:**

**TIF-1** was evacuated with supercritical  $\text{CO}_2$  in a Tousimis™ Samdri® PVT-30 critical point dryer. prior to drying, the DMF dispersed MOF sample was soaked in absolute ethanol (EtOH), replacing the soaking solution every 24 h for 72 h, to exchange the occluded solvent to EtOH. After the 72 h the exchange process was completed, the ethanol-containing samples were placed inside the dryer and the ethanol was exchanged with  $\text{CO}_{2(\text{L})}$  over a period of 6 h. During this time the liquid  $\text{CO}_2$  was vented under positive pressure for 5 minutes each hour. The rate of venting of  $\text{CO}_{2(\text{L})}$  was always kept below the rate of filling so as to maintain a full drying chamber. After 6 hr of venting and soaking with  $\text{CO}_{2(\text{L})}$  the chamber was sealed and the temperature was raised to 40°C. This brought the chamber pressure to around 1300 psi above the critical point of  $\text{CO}_2$ . The chamber was held above the critical point for 1 h at which point the chamber was slowly vented over the course of 15-18 h. The dried samples were placed in sealed containers and stored in a desiccator or immediately tested in  $\text{CO}_2$  physisorption.

#### **Procedure for MOF treatment in solvents:**

MOF sample was soaked in various organic solvents (DMF, acetone, ethanol, methanol and dichloromethane) for 12 h to evaluate the chemical stability. For PXRD measurements the solvent was decanted and the MOF sample was dried at 80 °C under vacuum. As shown by

PXRD results (Fig. S5), the MOF maintained the PXRD patterns and excellent crystallinity in all these solvents.

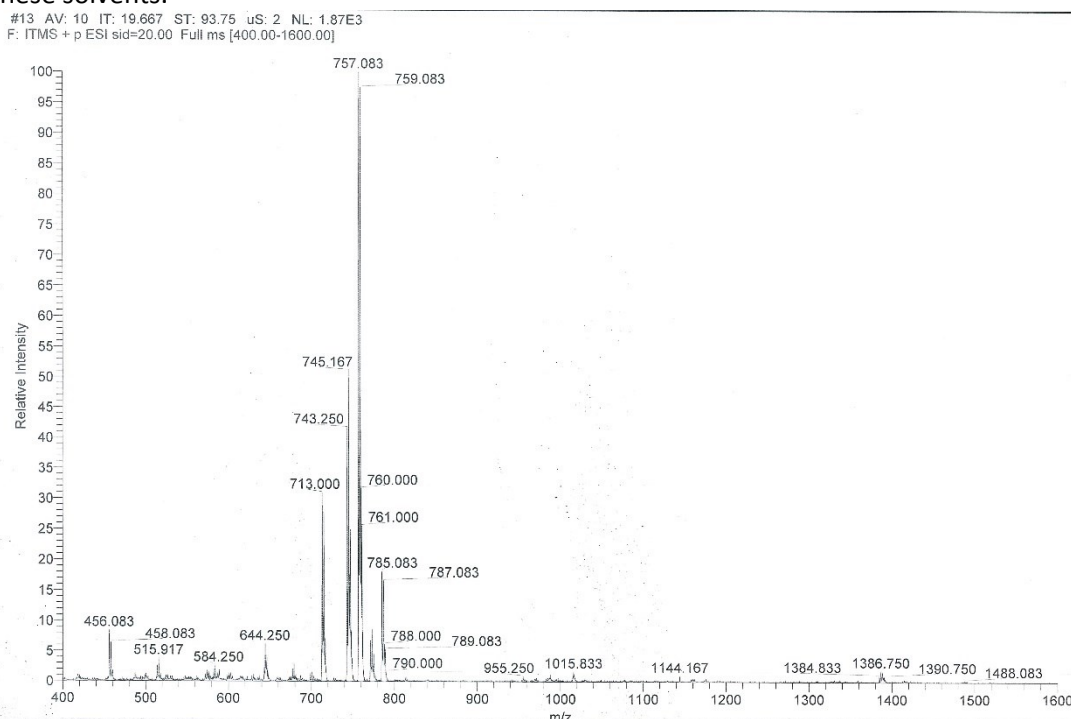


**Figure S1.** ESI-Mass Spectrum of linker  $\text{H}_2\text{L}^{2+}(\text{ClO}_4^-)_2$ .

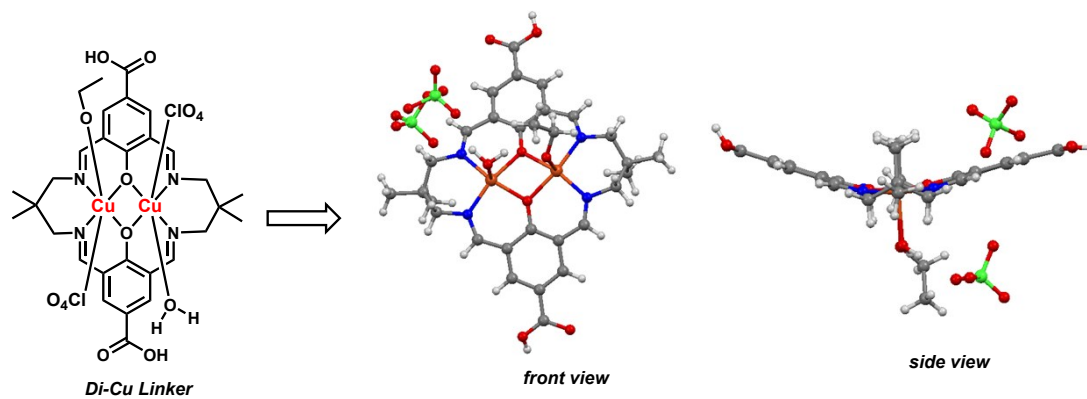
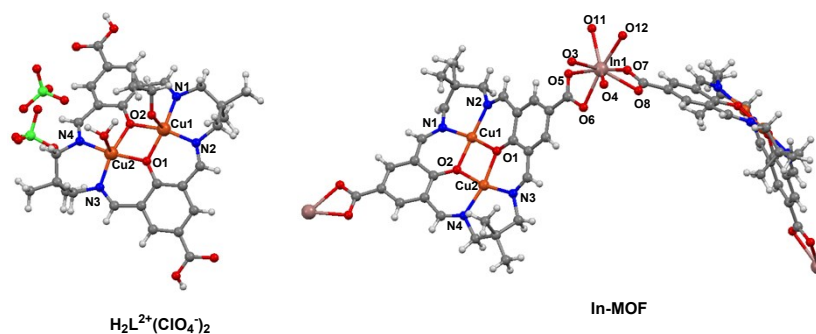


**Figure S2.** X-ray structure of dicopper Robson-type ligand  $\text{H}_2\text{L}^{2+}(\text{ClO}_4^-)_2$  and representing the bent side view of the linker.

**Table S1.** The coordination environment of  $\text{H}_2\text{L}^{2+}(\text{ClO}_4^-)_2$ , TIF-1 and selected labels for bond lengths (Å) and angles (°) list.



Complexes	$\text{H}_2\text{L}^{2+}(\text{ClO}_4^-)_2$	TIF-1
Bond lengths (Å)		
Cu1-O1	1.968(8)	1.964(9)
Cu1-O2	1.987(8)	1.981(9)
Cu1-O7	2.312(8)	-
Cu2-O1	1.985(7)	1.981(9)
Cu2-O2	1.976(8)	1.959(8)
Cu2-O8	2.227(9)	-
Cu1-N1	1.964(10)	1.946(11)
Cu1-N2	1.946(9)	1.926(13)
Cu2-N3	1.961(10)	1.963(11)
Cu2-N4	1.962(10)	1.982(12)
In1-O5	-	2.246(9)
In1-O6	-	2.280(8)
In1-O7	-	2.276(9)
In1-O8	-	2.294(8)
In1-O4	-	2.263(8)
In1-O3	-	2.260(9)
In1-O11	-	2.339(8)
In1-O12	-	2.261(9)
Bond angles (°)		
O1-Cu1-N2	92.00(3)	93.8(4)
N1-Cu1-N2	97.40(4)	94.6(5)
O2-Cu1-N1	93.20(3)	93.6(4)
O1-Cu2-N3	92.80(3)	92.0(4)
N3-Cu2-N4	97.80(4)	96.3(5)
O2-Cu2-N4	91.90(4)	94.1(4)
O2-Cu1-O1	76.3(3)	76.90(3)
O2-Cu2-O1	76.2(3)	77.00(4)
O5-In1-O6	-	57.7(3)
O7-In1-O8	-	58.1(3)
O5-C28-O6	-	119.5(12)
O7-C29-O8	-	121.5(13)

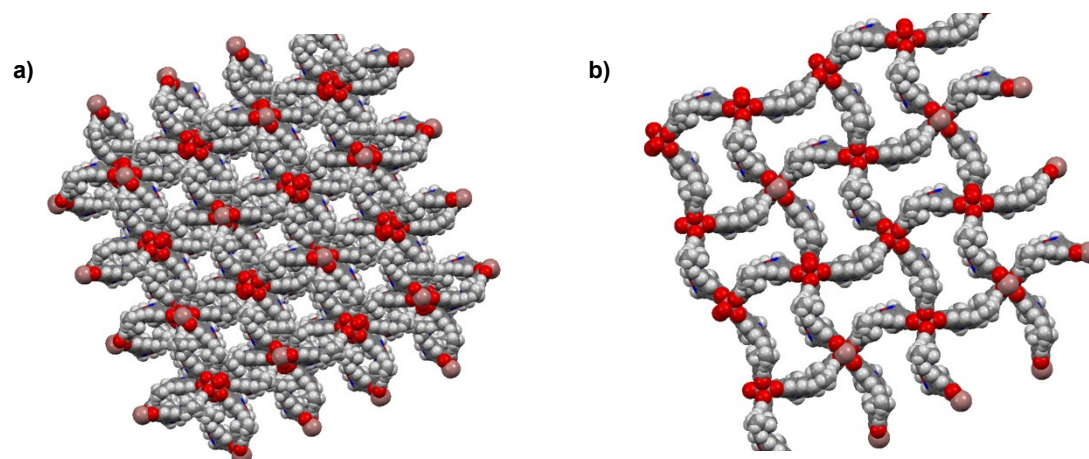


**Figure S3.** Space-filling diagram of a) 4-fold interpenetrated 3D network and b) single 3D network of TIF-1.

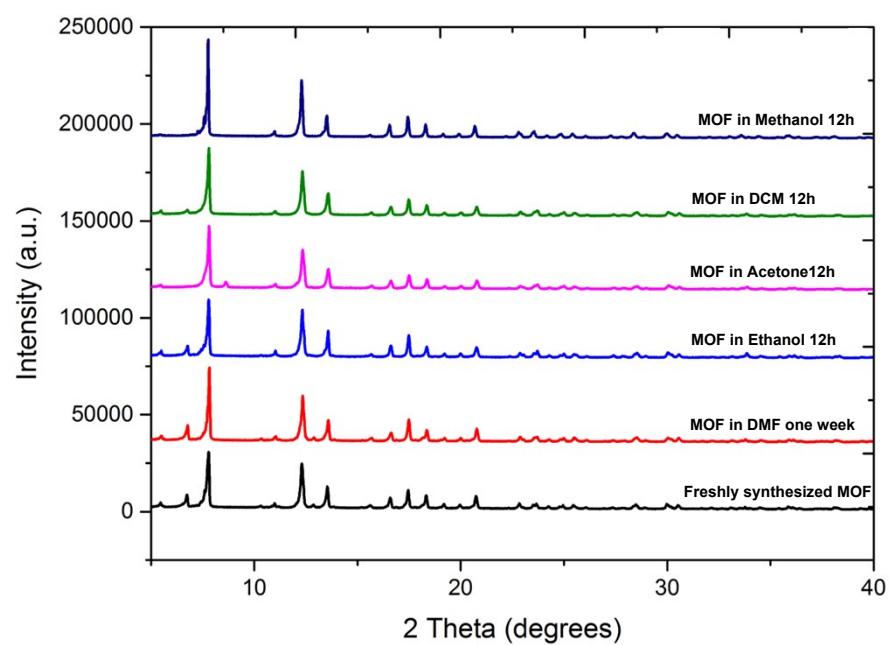


**Figure S4.** The stability of TIF-1 in different organic solvents.

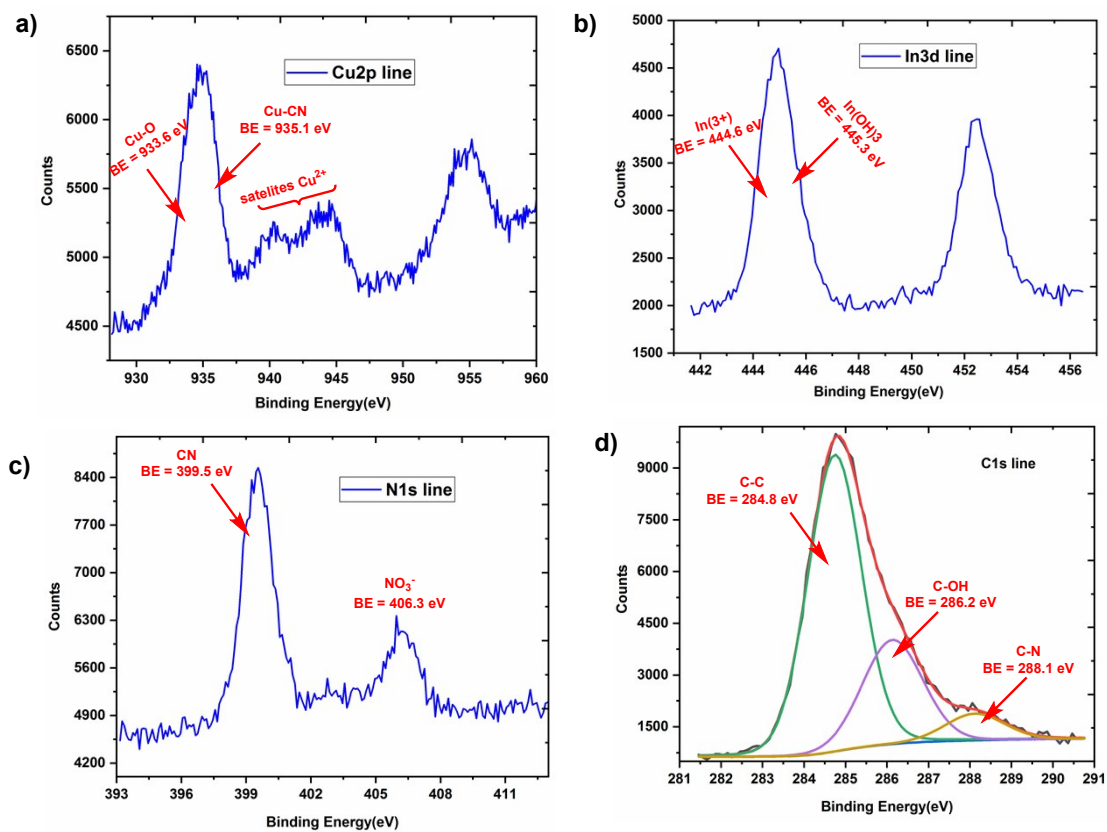


Figure S5. High resolution XPS of (a) Cu2p, (b) In3d, (c) N1s and (d) C1s lines for TIF-1 MOF.

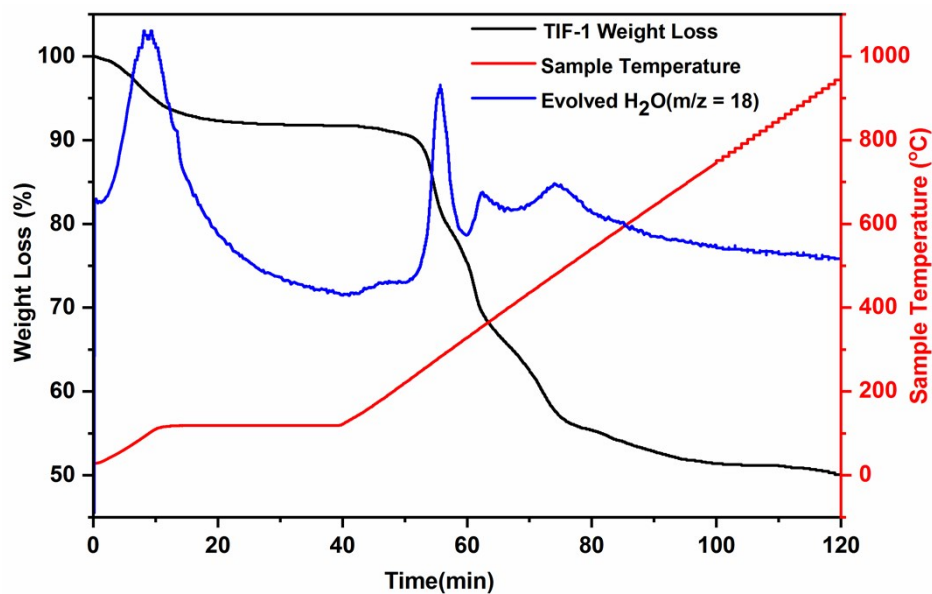
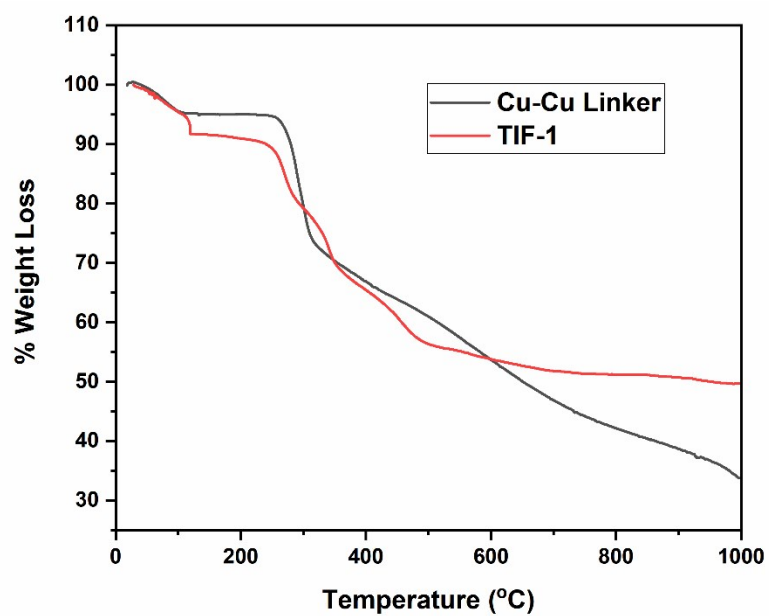
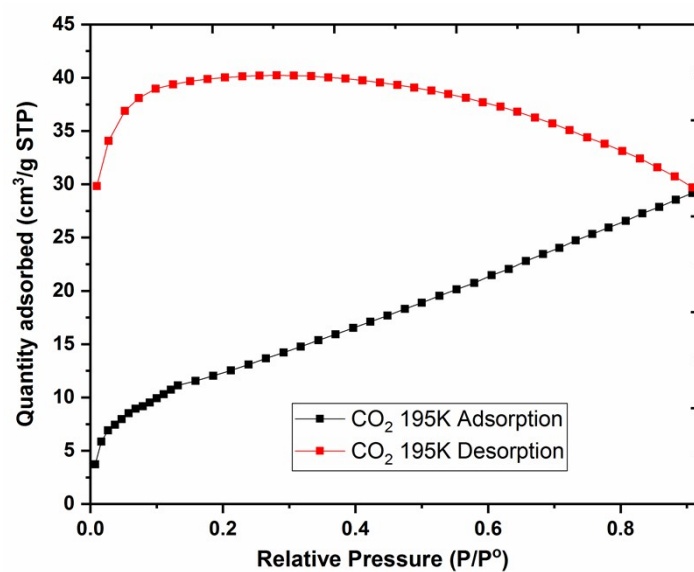


Figure S6. TGA-MS analysis of TIF-1.



**Figure S7.** TG curve of linker  $\text{H}_2\text{L}^{2+}(\text{ClO}_4^-)_2$  and TIF-1.



**Figure S8.** CO<sub>2</sub> adsorption isotherm at 195 K of TIF-1 after scCO<sub>2</sub> activation.



**References:**

1. T. Routasalo, J. Helaja, J. Kavakka and A. M. P. Koskinen, *Eur. J. Org. Chem.*, 2008, 3190-3199.
2. M. Zhou, Z. Ju and D. Yuan, *Chem. Commun.*, 2018, **54**, 2998-3001.
3. Dolomanov, O.V., Bourhis, L.J., Gildea, R.J., Howard, J.A.K. & Puschmann, H. (2009), *J. Appl. Cryst.* 42, 339-341.
4. Bourhis, L.J., Dolomanov, O.V., Gildea, R.J., Howard, J.A.K., Puschmann, H. (2015). *Acta Cryst.* A71, 59-75.
5. Sheldrick, G.M. (2015). *Acta Cryst.* C71, 3-8.
6. Mercury Software from CCDC: <http://www.ccdc.cam.ac.uk/Solutions/CSDSystem/Pages/Mercury.aspx>.
7. A. P. Nelson, O. K. Farha, K. L. Mulfort and J. T. Hupp, *Journal of the American Chemical Society*, 2009, **131**, 458-460.